

Measuring the level of nuclear activity in Seyfert galaxies and the unification scheme

Veeresh Singh^{1,2,*}, Prajval Shastri¹ and Guido Risaliti^{3,4}

¹ Indian Institute of Astrophysics, Bangalore 560034, India

² Department of Physics, University of Calicut, Calicut 673635, India

³ INAF-Osservatorio di Arcetri, Largo E. Fermi 5, I-50125 Firenze, Italy

⁴ Harvard-Smithsonian Center for Astrophysics, 60 Garden St. Cambridge, MA 02138, USA

Received xxxx xx, xxxx; accepted xxxx xx, xxxx

ABSTRACT

Context. The unification scheme of Seyfert galaxies hypothesizes that Seyfert type 1s and type 2s are intrinsically similar and the observed differences between the two subtypes are solely due to the differing orientations of toroidal-shaped obscuring material around the AGN. In the framework of the unification scheme, both the Seyfert subtypes are expected to show similar intrinsic nuclear properties, such as the absorption-corrected AGN X-ray luminosity, bolometric luminosity, accretion rate and the mass of the supermassive black hole.

Aims. To test the predictions of the Seyfert unification scheme, we make statistical comparison of the distributions of: (i) the absorption-corrected 2.0 - 10 keV X-ray luminosities, (ii) the bolometric luminosities, (iii) the black hole masses and, (iv) the Eddington ratios, of Seyfert type 1s and type 2s.

Methods. We use an optically selected Seyfert sample in which type 1s and type 2s are matched in properties that are independent to the orientation of the obscuring torus, the AGN axis and the host galaxy.

Results. The distributions of the absorption-corrected 2.0 - 10 keV X-ray luminosities ($L_{2.0-10\text{ keV}}^c$), the bolometric luminosities (L_{Bol}), the black masses (M_{BH}) and, the Eddington ratios (λ) are statistically similar for the two Seyfert subtypes, consistent with the orientation and obscuration based Seyfert unification scheme. The Eddington ratio distributions suggest that both the Seyfert subtypes are accreting at sub-Eddington level with wide span of Eddington ratios *i.e.*, 10^{-4} - 10^{-1} .

Key words. Galaxies: Seyfert – X-rays: galaxies – Galaxies: active

1. Introduction

Seyfert galaxies are categorized as nearby, low-luminosity, radio-quiet AGNs powered by accretion onto supermassive black holes. Seyfert galaxies are classified mainly into two subclasses named as type 1 and type 2, based on the presence and absence of broad emission lines in their optical spectra, respectively (Antonucci 1993). Seyfert unification scheme hypothesizes that the two subtypes are intrinsically similar *i.e.*, belong to the same parent population and appear different solely due to the differing orientations of the obscuring material having toroidal geometry around the AGN. When the plane of the obscuring torus is along the observer's line-of-sight *i.e.*, edge-on view (type 2s), the central engine and broad line region clouds are hidden, while in pole-on view (type 1s) the central engine as well as broad line region clouds are directly seen (Antonucci & Miller 1985; Antonucci 1993; Urry et al. 1995).

There have been several attempts to investigate the validity of Seyfert unification scheme, giving both consistent as well as inconsistent results. Results such as the presence of broad emission lines in the polarized optical and infrared spectra of many Seyfert 2s (Moran et al. 2000), the biconical structure of the narrow line region (Wilson 1996), systematically higher X-ray absorbing column density in Seyfert type 2s (Cappi et al. 2006) and similar nuclear radio properties of both the subtypes (Lal et al. 2011) are consistent with the unification scheme. While, results such as the absence of hidden Seyfert 1 nuclei in several

Seyfert 2s (Tran 2001, 2003), Seyfert 1s being preferentially hosted in galaxies of earlier Hubble type (Malkan et al. 1998), lack of X-ray absorption in some Seyfert 2s (Panessa & Bassani 2002), and Seyfert 2s having a higher propensity of nuclear starbursts (Buchanan et al. 2006) are inconsistent with the unification scheme. Sample selection is arguably the most important issue in testing the predictions of Seyfert unification scheme and several results inconsistent to the scheme can be explained as due to the biases inherent in the samples (Antonucci 2002). Indeed, it has been shown that the Seyfert samples selected from optical and UV surveys tend to be biased against obscured and faint sources (Ho & Ulvestad 2001). The obscuring torus absorbs the optical, UV photons emanating from AGN and reradiates in IR. Also, emission at IR wavelengths does not suffer large extinction, therefore, IR selected samples are likely to be less susceptible to selection biases (Spinoglio & Malkan 1989). However, IR selected samples can be biased towards unusually dusty and sources with higher level of nuclear star formation (Buchanan et al. 2006). Seyfert samples selected from X-ray surveys have also been used to test the predictions of the Seyfert unification (Awaki et al. 1991; Smith & Done 1996; Turner et al. 1997; Bassani et al. 1999). However, studies based on [OIII] selected samples have shown that the X-ray ($E < 10$ keV) selected samples are biased against heavily obscured AGNs (Risaliti et al. 1999; Heckman et al. 2005). Hard X-ray photons can transmit through the obscuring material and therefore, samples based on hard X-ray surveys are expected to be least biased. However, Seyfert samples based on *INTEGRAL* and

* veeresh@iiap.res.in

Swift/BAT surveys preferentially contain relatively large number of high luminosity and less absorbed Seyferts (Tueller et al. 2008; Treister et al. 2009; Beckmann et al. 2009), possibly due to less effective area which limits the sensitivity only to bright sources ($\sim 10^{-11}$ erg s $^{-1}$ cm $^{-2}$). Therefore, samples based on hard X-ray surveys are likely to be biased against heavily obscured Compton-thick and low luminosity AGNs (Heckman et al. 2005; Wang et al. 2009). Thus, in general, samples derived from flux limited surveys tend to bias against obscured and faint sources. The quest of testing the validity and limitations of Seyfert unification scheme with more improved and well defined samples continues (*e.g.*, Cappi et al. (2006); Dadina (2008); Horst et al. (2008); Ricci et al. (2011); Brightman & Nandra (2011)), however, issues related to the sample selection still remain. It has been argued that the samples based on the properties that are independent to the orientation of the obscuring torus are more appropriate to test the unification scheme (Schmitt et al. 2003; Lal et al. 2011; Singh et al. 2011). Such samples are less prone to the biases that are generally inherent in the samples derived from flux limited surveys. Lal et al. (2011) have presented a Seyfert sample based on orientation-independent properties and the two Seyfert subtypes of this sample are matched in the orientation-independent properties. Keeping above sample selection issues in mind, we use Lal et al. (2011) sample with the aim to test the Seyfert unification scheme by making statistical comparison of the distributions of nuclear properties such as the absorption-corrected 2.0 - 10 keV X-ray luminosities ($L_{2.0-10\text{ keV}}^c$), the bolometric luminosities (L_{Bol}), the black hole masses (M_{BH}) and the Eddington ratios (λ) of the Seyfert type 1s and type 2s.

The structure of this paper is as following. In section 2, we discuss the sample details. In section 3, we discuss the empirical relations that we used to derive the bolometric luminosities of the sample sources. A brief note on Eddington ratios is given in section 4. In section 5, we discuss the comparisons of the absorption-corrected luminosities, the bolometric luminosities, the black hole masses and the Eddington ratios of the two Seyfert subtypes. Throughout the paper we have assumed cosmological parameters $H_0 = 71$ km $^{-1}$ Mpc $^{-1}$, $\Lambda_m = 0.27$, and $\Lambda_{\text{vac}} = 0.73$.

2. The sample

We use the Seyfert sample of Lal et al. (2011) that is consist of 20 (10 type 1s and 10 type 2s) Seyfert galaxies. In this sample, Seyfert galaxies are defined as radio-quiet ($\frac{F_{\text{S GHz}}}{F_{\text{B-band}}} < 10$; Kellermann et al. (1989)), low optical luminosity AGN ($M_B > -23$; Schmidt & Green (1983)), hosted in spiral or lenticular galaxies (Weedman 1977). The sample selection is based on the properties that do not depend on the orientation of the obscuring torus, the AGN axis and the host galaxy. The orientation-independent properties used for the sample selection are: cosmological redshift, [OIII] $\lambda 5007\text{\AA}$ line luminosity, Hubble stage of the host galaxy, absolute stellar magnitude of the host galaxy and absolute bulge magnitude. All these properties are also intimately linked to the evolution of AGN as well as host galaxy. The sample is selected such that the two Seyfert subtypes have matched distributions in the orientation-independent properties. We refer readers to see Lal et al. (2011) for greater details on the sample selection. The sample was formulated to study the nuclear radio properties of Seyferts and is constrained by the Very Large Baseline Interferometer (VLBI) observing feasibility. Lal et al. (2011) noted that 54 Seyferts met VLBI observing feasibility criterion and 29 of these 54 had all the required

orientation-independent parameters in the literature. From these 29, they picked 20 Seyferts such that the two Seyfert subtypes had matched distributions in the orientation-independent parameters. The sources which were deviating in matching the distributions of the orientation-independent parameters were left out. In other words, the two Seyfert subtypes should lie within the same range of values for a given parameter to enter into the sample. Also, it was ensured that in a given bin of a parameter distribution, type 1s do not outnumber the type 2s and vice-versa. Indeed, the selected 20 Seyferts are not unique or complete in any aspect. Nevertheless, the sample is sufficiently qualified to test the predictions of Seyfert unification scheme at any wavelength regime since it is based on the orientation-independent properties, and ensure that the two Seyfert subtypes are intrinsically similar within the framework of the unification scheme. Furthermore, it is possible to enlarge the sample size by relaxing the VLBI observing feasibility criterion, but keeping the criterion of similar distributions for the two Seyfert subtypes in the orientation-independent parameters, intact. However, we emphasize that the more important issue is the sample selection and not the sample size.

The criterion of similar distributions of the orientation-independent parameters for the two subtypes and VLBI observing feasibility may introduce a positive bias towards the sources having similar AGN and host galaxies properties. Therefore, this sample may not be claimed as a complete representative of the entire class of Seyfert galaxies. However, more importantly, matched distributions are essential to ensure that we are not comparing entirely intrinsically different sources selected from different parts of the evolution function (luminosity, bulge mass, Hubble type, redshift). Since the AGN and host galaxy properties are likely to affect the AGN surrounding environment *e.g.*, opening angle of the obscuring torus decreases with the increase in AGN luminosity (Ueda et al. 2003; Hasinger 2008), formation of BLR clouds may depend on the AGN luminosity (Laor 2003; Nicastro 2000), in low luminosity AGNs accretion rate increases from early-type to late-type galaxies (Ho 2009). Therefore, the samples that have large variations in the AGN and host galaxy properties are expected to show the effect of these variations in the observed properties other than the differences owing to the differing orientations of the obscuring torus. Lal et al. (2011) Seyfert sample based on the matched distributions of the orientation-independent parameters, minimizes the impact of differences caused by the differing properties of the AGN as well as host galaxy.

Using the same sample we have shown in our previous paper (Singh et al. (2011), hereafter paper-I) that the comparisons of X-ray properties *e.g.*, distributions of the observed X-ray luminosities, the absorbing column densities, the equivalent widths of Fe $K\alpha$ line and the flux ratios of 2.0 - 10 keV hard X-ray to [OIII] line emission of the two Seyfert subtypes, are consistent with the Seyfert unification scheme.

3. Estimating bolometric luminosity

In order to calculate the bolometric luminosity of a source one requires complete spectral energy distribution (SED) of the source over the entire electromagnetic spectrum. However, in practice complete SED is not available for most of the AGNs. In the literature, both nuclear 2.0 - 10 keV X-ray luminosity as well as [OIII] $\lambda 5007\text{\AA}$ line luminosity have been used to estimate the bolometric luminosity (Heckman et al. 2005; Kauffmann & Heckman 2009; Lamastra et al. 2009). In follow-

ing subsections we discuss the empirical relations that we use to estimate the bolometric luminosities for our sample sources.

3.1. Using X-ray luminosity

Different studies in the literature have suggested different correction factors to estimate the bolometric luminosity from the 2.0 - 10 keV X-ray luminosity (Elvis et al. 1994; Ho 2008). However, SED of an AGN vary with accretion rate and therefore it may not be appropriate to use a single correction factor to estimate the bolometric luminosity (L_{Bol}) from the nuclear X-ray luminosity ($L_{2.0-10 \text{ keV}}$). We estimated the bolometric luminosity from absorption-corrected 2.0 - 10 keV X-ray luminosity using the empirical relation given in Marconi et al. (2004).

$$\log\left(\frac{L_{\text{Bol}}}{L_{2.0-10 \text{ keV}}^c}\right) = 1.54 + 0.24\mathcal{L} + 0.012\mathcal{L}^2 - 0.0015\mathcal{L}^3 \quad (1)$$

where $\mathcal{L} = \log L_{\text{Bol}} - 12$, and L_{Bol} , $L_{2.0-10 \text{ keV}}^c$ are in units of L_{\odot} . Marconi et al. (2004) derived this bolometric correction using an average intrinsic spectral energy distribution template for radio-quiet AGNs and also accounted for the variations in AGN SEDs by using the well-known anti-correlation between the optical-to-X-ray spectral index (α_{OX}) and 2500 Å luminosity. We obtain the absorption-corrected 2.0 - 10 keV X-ray luminosities ($L_{2.0-10 \text{ keV}}^c$) of our sample sources using the 0.5 - 10 keV *XMM-Newton* X-ray spectral fits (see, Paper-I). For Compton-thin sources, the absorbing column densities are accurately known and thus the absorption-corrected fluxes/luminosities can be obtained by fixing the equivalent hydrogen column density (N_{H}) equal to '0' in the best X-ray spectral fitting models. However, the correction for X-ray absorption in case of the Compton-thick sources is non-trivial since photoelectric absorption cut-off and hence absorbing column density is not measurable by the X-ray observations that are limited up to 10 keV, e.g., *XMM-Newton*, *Chandra* and *ASCA* observations. In order to get the absorption-corrected X-ray fluxes for Compton-thick sources we have used flux diagnostic ratio which is based on measuring the X-ray flux against [OIII] $\lambda 5007\text{\AA}$ flux, i.e., $R_x = \frac{F_{2.0-10.0 \text{ keV}}}{F_{\text{[OIII]}}}$ (Bassani et al. 1999; Panessa et al. 2006). We estimate the absorption-corrected 2.0 - 10.0 keV X-ray flux/luminosity for a Compton-thick source by multiplying the observed flux/luminosity with a correction factor f_{cor} that is approximated as the ratio of the medians of $R_{x\text{Compton-thin}}$ to $R_{x\text{Compton-thick}}$ (i.e., $f_{\text{cor}} = \frac{R_{x\text{Compton-thin, median}}}{R_{x\text{Compton-thick, median}}}$, González-Martín et al. (2009)), where $R_{x\text{Compton-thin}}$ is $\frac{F_{(2.0-10.0 \text{ keV})\text{cor}}}{F_{\text{[OIII]}\text{cor}}}$ (i.e., the ratio of the absorption-corrected 2.0 - 10.0 keV flux to the reddening corrected [OIII] $\lambda 5007\text{\AA}$ flux for a Compton-thin source), while $R_{x\text{Compton-thick}}$ is $\frac{F_{(2.0-10.0 \text{ keV})\text{obs}}}{F_{\text{[OIII]}\text{cor}}}$ (i.e., the ratio of the observed 2.0 - 10.0 keV flux to the reddening corrected [OIII] $\lambda 5007\text{\AA}$ flux for a Compton-thick source). In paper-I we report that in our sample of 20 Seyferts, 7/10 type 2 Seyferts are Compton-thick and 13 Seyferts (10 type 1s and 3 type 2s) are Compton-thin. Using the median values of $R_{x\text{Compton-thin}}$ and $R_{x\text{Compton-thick}}$ in this sample, we estimated the absorption correction factor $f_{\text{cor}} \sim 70$, which is close to the one reported in Panessa et al. (2006) by using similar flux diagnostic method but considering the flux ratios of Seyfert type 1s and type 2s rather than that of Compton-thick and Compton-thin sources. We caution that the true value of the correction factor (f_{cor}) may be different for different sources depending upon the true value of the absorbing column density. Moreover, we note that our approximated

value for the correction factor F_{cor} is not too different than that for the typical Compton-thick Seyferts (Levenson et al. 2006; Brightman & Nandra 2011) and therefore, it is unlikely to affect our analysis statistically.

3.2. Using [OIII] $\lambda 5007\text{\AA}$ line luminosity

The [OIII] $\lambda 5007\text{\AA}$ line emission originates in the narrow line region and its luminosity correlates with the total AGN power (Mulchaey et al. 1994; Heckman et al. 2005). Also unlike X-ray emission which can be heavily absorbed (e.g., in Compton-thick AGNs), [OIII] line emission is not much affected by dust obscuration from the torus since it originates in the narrow line region which lies outside the torus. Heckman et al. (2004) reported that for type 1 Seyfert nuclei the average bolometric correction to the extinction uncorrected [OIII] luminosity is $(L_{\text{Bol}}/L_{\text{[OIII]}}) \sim 3500$, with a variance of 0.38. However, extinction for the [OIII] emission caused by dust present in NLR itself can be substantial and therefore extinction-corrected [OIII] luminosity ($L_{\text{[OIII]}}^c$) is a more direct indicator of the nuclear luminosity. To estimate the bolometric luminosity from the [OIII] line luminosity we have used the correction factors given in Lamastra et al. (2009) that are estimated by following a method similar to Heckman et al. (2004), but using the extinction-corrected [OIII] luminosity instead of the observed one. Lamastra et al. (2009) reported the luminosity dependent bolometric correction factors ($C_{\text{[OIII]}}$) 87, 142, 454 for the [OIII] luminosity ranges $\log L_{\text{[OIII]}} = 38 - 40$, $40 - 42$, $42 - 44$, respectively. The luminosity-dependent [OIII] correction factors ($C_{\text{[OIII]}}$) are obtained by using $L_X - L_{\text{[OIII]}}^c$ correlation fit and the luminosity-dependent X-ray bolometric correction of Marconi et al. (2004). For the sources which do not have extinction-corrected [OIII] luminosities we have used Heckman et al. (2004) relation to derive the bolometric luminosities.

4. Eddington ratio

Eddington luminosity ($L_{\text{Edd}} \simeq 1.3 \times 10^{38} (M_{\text{BH}}/M_{\odot})$) is an upper limit of the luminosity produced by a black hole of mass M_{BH} . The Eddington limit is a physical limit at which the outward radiation pressure from the accreting matter balances the inward gravitational pressure exerted by the black hole. The mass accretion rate can be parametrized by Eddington ratio ($\lambda = L_{\text{Bol}}/L_{\text{Edd}}$) that is the ratio of the bolometric luminosity (L_{Bol}) to the Eddington luminosity (L_{Edd}) for a given black hole mass (M_{BH}). The Eddington ratio can be expressed as

$$\lambda = \frac{L_{\text{bol}}}{L_{\text{Edd}}} \simeq 0.1 \left(\frac{L_{\text{bol}}}{1.4 \times 10^{44} \text{ erg s}^{-1}} \right) \left(\frac{M_{\text{BH}}}{10^7 M_{\odot}} \right) \quad (2)$$

(Wang & Zhang 2007). For all of our sample sources (except for MRK 1218), the estimated black hole mass is available in the literature. The black hole masses are estimated using different methods such as reverberation mapping, $M-\sigma$ relation (Gebhardt et al. 2000; Ferrarese & Merritt 2000). In order to calculate Eddington ratio, we need bolometric luminosity (L_{Bol}) that we estimate using the absorption-corrected 2.0 - 10 keV X-ray luminosity as well as the [OIII] line luminosity. Thus, for a source, we have two values of the Eddington ratio, one is λ_X , where L_{Bol}^X is used for the bolometric luminosity and the other one is $\lambda_{\text{[OIII]}}$, where $L_{\text{Bol}}^{\text{[OIII]}}$ is used for the bolometric luminosity. Figure 3 shows that the bolometric luminosities obtained from the X-ray (L_{Bol}^X) and the [OIII] luminosities ($L_{\text{Bol}}^{\text{[OIII]}}$) are similar. There are three sources (i.e., MRK 231, MRK 1 and NGC

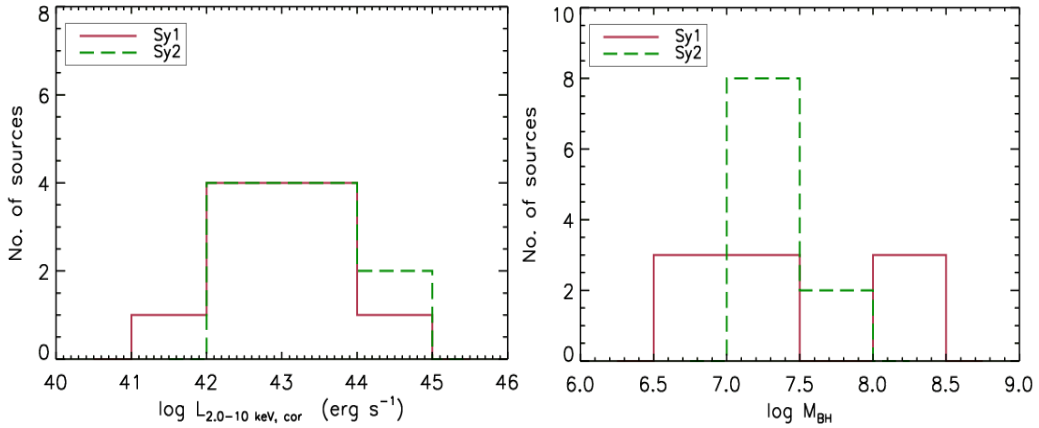
Table 1. Absorption-corrected 2.0 - 10 keV X-ray luminosities, bolometric luminosities, black hole masses and Eddington ratios for two Seyfert subtypes.

Name	Seyfert type	$\log L_{2.0-10 \text{ keV}}^c$ (erg s^{-1})	$\log L_{[\text{OIII}]}^c$ (erg s^{-1})	$\log L_{\text{Bol}}^x$ (erg s^{-1})	$\log L_{\text{Bol}}^{[\text{OIII}]}$ (erg s^{-1})	$\log M_{\text{BH}}$ (M_{\odot})	Ref	$\log \lambda_x$	$\log \lambda_{[\text{OIII}]}$
MCG+8-11-11	1	43.79	42.43	45.25	45.09	8.06	6	-1.92	-2.09
MRK 1218	1	42.69	41.61	43.87	43.76
NGC 2639	1	41.92	40.86	42.94	43.02	8.02	3	-4.20	-4.12
NGC 4151	1	42.40	41.39	43.51	43.54	7.18	2	-2.79	-2.75
MRK 766	1	42.50	41.84	43.62	43.99	6.64	4	-2.13	-1.76
MRK 231	1	42.53	41.96 [†]	43.66	45.51	7.24	5	-2.69	-0.85
ARK 564	1	43.37	41.38 [†]	44.71	44.93	6.50	4	-0.91	-0.69
NGC 7469	1	43.45	42.96	44.82	45.62	6.84	7	-1.14	-0.34
MRK 926	1	44.20	42.25 [†]	45.79	45.79	7.14	6	-0.47	-0.46
MRK 530	1	43.70	40.98 [†]	45.14	44.53	8.08	7	-2.06	-2.67
MRK 348	2	43.45	42.19	44.81	44.85	7.21	7	-1.51	-1.47
MRK 1	2	42.50	42.39	43.63	45.04	7.16	7	-2.64	-1.23
NGC 2273	2	42.74	41.16	43.92	43.82	7.30	7	-2.50	-2.60
MRK 78	2	44.09	43.29	45.64	45.94	7.87	7	-1.34	-1.04
NGC 5135	2	42.68	42.42	43.85	45.08	7.35	1	-2.62	-1.39
MRK 477	2	44.44	43.44	46.11	46.10	7.20	1	-0.21	-0.22
NGC 5929	2	42.04	40.98	43.07	43.64	7.25	7	-3.29	-2.72
NGC 7212	2	43.90	42.80	45.39	45.46	7.47	1	-1.19	-1.12
MRK 533	2	43.91	42.64	45.41	45.30	7.56	7	-1.27	-1.38
NGC 7682	2	43.07	41.76	44.33	44.42	7.28	7	-2.06	-1.98

Notes: Col. (1), source name; col. (2), Seyfert subtype; col. (3), absorption-corrected 2.0 - 10 keV X-ray luminosity; col. (4), extinction-corrected [OIII] luminosity; col. (5), bolometric luminosity derived from 2.0 - 10 keV X-ray luminosity; col. (6), bolometric luminosity derived from [OIII] line luminosity; col. (7), black hole masses; col. (8), references for black hole masses; col. (9) Eddington ratio where the estimated bolometric luminosity is derived from X-ray luminosity; col. (10), Eddington ratio where the estimated bolometric luminosity is derived from [OIII] line luminosity.

[†] : [OIII] luminosity is uncorrected for extinction as the Balmer decrement value is unavailable.

References- 1: Bian & Gu (2007), 2: Kaspi et al. (2000), 3: McElory (1995), 4: Merloni et al. (2003), 5: Dasyra et al. (2006), 6: Wang & Zhang (2007), 7: Woo & Urry (2002).

**Fig. 1.** *Left:* Distributions of the absorption-corrected 2.0 - 10 keV X-ray luminosities ($L_{2.0-10 \text{ keV}}$) for the two Seyfert subtypes. *Right:* Distribution of the black hole masses (in M_{\odot} units) for the two Seyfert subtypes.

5135) which show more than one order of magnitude difference between L_{Bol}^x and $L_{\text{Bol}}^{[\text{OIII}]}$. One possible reason for it may be that $L_{\text{Bol}}^{[\text{OIII}]}$ values for these sources are overestimated due to large scatter involved in $L_{[\text{OIII}]}^c - L_{\text{Bol}}$ relation *i.e.*, in bolometric correction factor $C[\text{OIII}]$ (Lamastra et al. 2009). Starburst contamination to $L_{[\text{OIII}]}$ may also attribute to the overestimation of $L_{\text{Bol}}^{[\text{OIII}]}$ as some of these sources *e.g.*, MRK 231 (Taylor et al. 1999), NGC 5135 (González Delgado et al. 1998) are known to host circumnuclear starburst. Furthermore, $L_{[\text{OIII}]}$ is only an indirect estimator of the nuclear luminosity and it depends on various factors such as on the geometry of the system, on the amount

of gas, and on any possible shielding effect that may affect the ionizing radiation seen by the NLR.

5. Discussion

Table 1 lists the absorption-corrected 2.0 - 10 keV X-ray luminosities ($L_{2.0-10 \text{ keV}}^c$), the extinction-corrected [OIII] 5007 Å line luminosities ($L_{[\text{OIII}]}^c$), the bolometric luminosities derived from the X-ray as well as the [OIII] luminosities (L_{Bol}^x , $L_{\text{Bol}}^{[\text{OIII}]}$), the black hole masses (M_{BH}) and the Eddington ratios (λ_x , $\lambda_{[\text{OIII}]}$) for the Seyfert type 1s and type 2s of our sample. In following subsections we discuss the statistical comparisons of the nuclear

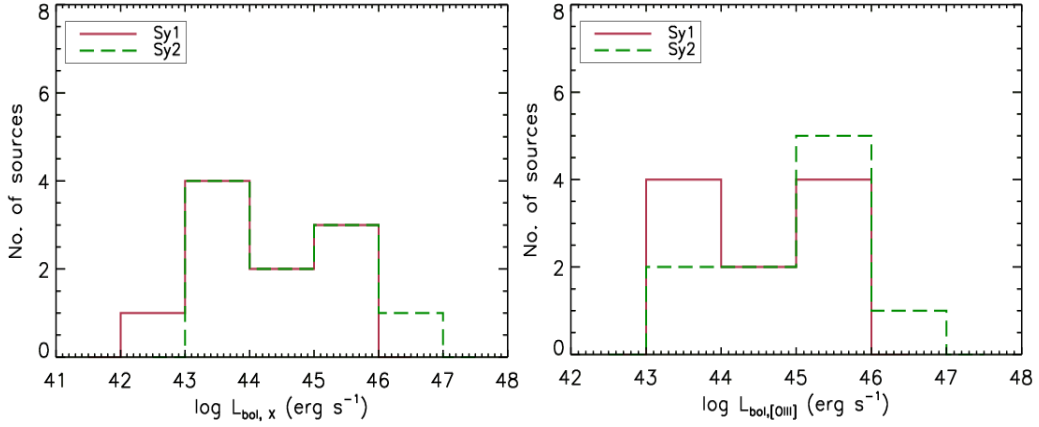


Fig. 2. Distributions of the bolometric luminosities (L_{Bol}) for the two Seyfert subtypes. *Left:* L_{Bol} is derived from $L^c_{2.0-10 \text{ keV}}$, *Right:* L_{Bol} is derived from $L_{[\text{OIII}]}$.

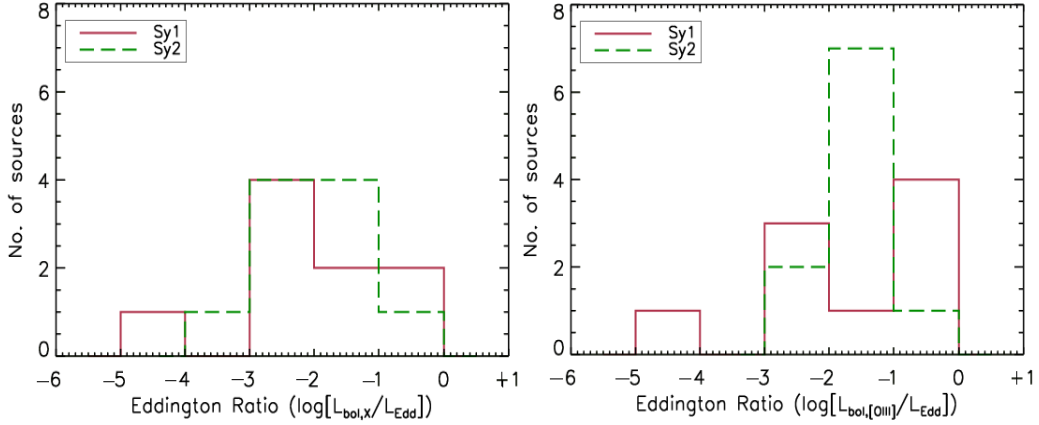


Fig. 4. Distributions of the Eddington ratios for the two Seyfert subtypes. *Left:* L_{Bol} is derived from $L^c_{2.0-10 \text{ keV}}$, *Right:* L_{Bol} is derived from $L_{[\text{OIII}]}$.

Table 2. Medians and Kolmogorov-Smirnov two sample tests for the statistical comparison of various distributions of the two Seyfert subtypes

Distribution	Median		D	p value
	Type 1s	Type 2s		
$\log L^c_{0.5-2.0 \text{ keV}}$	43.15	43.30	0.3	0.79
$\log L^x_{\text{Bol}}$	44.47	44.63	0.3	0.79
$\log L^{\text{[OIII]}}_{\text{Bol}}$	44.64	45.01	0.2	0.99
$\log M_{\text{BH}}$	7.18	7.29	0.5	0.16
$\log \lambda_X$	-2.06	-1.70	0.2	0.98
$\log \lambda_{[\text{OIII}]}$	-1.76	-1.38	0.3	0.75

Kolmogorov - Smirnov two sample test examines the hypothesis that two samples comes from same distribution. $D = \sup x |S1(x) - S2(x)|$ is the maximum difference between the cumulative distributions of two samples $S1(x)$ and $S2(x)$, respectively.

properties of the two Seyfert subtypes with the primary aim to examine the validity of Seyfert unification scheme.

5.1. Comparison of absorption-corrected 2.0 - 10 keV X-ray luminosities

In the unification scenario, the X-ray emitting AGN in Seyfert type 2s is viewed through the obscuring torus and therefore Seyfert type 2s are expected to show lower observed 2.0 - 10 keV X-ray luminosities than type 1s as long as the obscuring

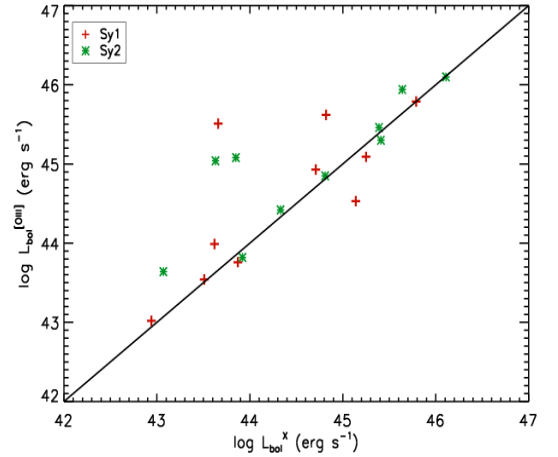


Fig. 3. Comparison of the bolometric luminosities (L_{Bol}) obtained from $L^c_{2.0-10 \text{ keV}}$ and $L_{[\text{OIII}]}$ respectively. The solid line represents $L^x_{\text{Bol}} = L^{[\text{OIII}]}_{\text{Bol}}$ line.

column density is sufficiently high ($N_{\text{H}} > 10^{22} \text{ cm}^{-2}$). We have shown in paper-I that the Seyfert type 2s compared to type 1s, show systematically lower observed soft (0.5 - 2.0 keV) and hard (2.0 - 10 keV) X-ray luminosities, consistent with the unification scheme. Since the differences between the two Seyfert sub-

types are due to the differing orientations of the obscuring torus and therefore if 2.0 - 10 keV X-ray luminosities are corrected for the line-of-sight absorption, both Seyfert type 1s and type 2s are expected to show similar 2.0 - 10 keV luminosity distributions. Figure 1 shows the 2.0 - 10 keV absorption-corrected X-ray luminosity distributions for the two Seyfert subtypes of our sample. In our sample, the type 1s have $L_{2.0-10\text{ keV}}^c$ in the range of $\sim 8.3 \times 10^{41}$ to $\sim 1.6 \times 10^{44}$ erg s $^{-1}$ with the median value $\sim 1.5 \times 10^{43}$ erg s $^{-1}$, while for type 2s, $L_{2.0-10\text{ keV}}^c$ ranges from $\sim 1.1 \times 10^{42}$ to $\sim 2.8 \times 10^{44}$ erg s $^{-1}$ with the median value $\sim 2.0 \times 10^{43}$ erg s $^{-1}$. The two sample KS test confirms that the Seyfert type 1s and type 2s have similar 2.0 - 10 keV absorption-corrected X-ray luminosity distributions, consistent with the unification scheme. The KS test shows that there is $\sim 79\%$ probability that the $L_{2.0-10\text{ keV}}^c$ distributions of type 1 and type 2 Seyferts are drawn from the same parent population (Table 2). The absorption-corrected 2.0 - 10 keV X-ray luminosities for our sample Seyferts are similar to the ones reported in the previous studies (Cappi et al. 2006). The absorption-corrected 2.0 - 10 keV X-ray luminosity can be considered as the representative of AGN power as long as the X-ray photons in the 2.0 - 10 keV band are not substantially diminished by other than photo-electric absorption and are not contaminated by non-AGN emission. Circumnuclear starburst is reported to be present in some of our sample sources (*e.g.*, MRK 477, (Heckman et al. 1997); NGC 5135, (González Delgado et al. 1998)), however, it has been argued that the circumnuclear starburst mainly contribute to the soft X-ray 0.5 - 2.0 keV band and its contamination to 2.0 - 10 keV energy band is not substantial (Levenson et al. 2004).

5.2. Comparison of AGN bolometric luminosities

The bolometric luminosity of AGN represents the rate of energy emitted over the entire electromagnetic waveband by the accreting black hole. AGN bolometric (L_{Bol}) depends on the mass accretion rate and the radiative efficiency of the accreting matter. Therefore, if Seyfert type 1s and type 2s are intrinsically similar as hypothesized by the unification scheme, then both the subtypes should show similar distributions of the bolometric luminosity. As discussed in the section 3, we have estimated the bolometric luminosities of our sample sources using the absorption-corrected 2.0 - 10 keV X-ray luminosity as well as the [OIII] line luminosity. Figure 2 shows the distributions of bolometric luminosities (L_{Bol}^X and $L_{\text{Bol}}^{[\text{OIII}]}$) for the Seyfert type 1s and type 2s. In our sample, Seyfert type 1s have L_{Bol}^X ranging from $\sim 8.7 \times 10^{42}$ to $\sim 6.2 \times 10^{46}$ erg s $^{-1}$ with the median value $\sim 3.0 \times 10^{44}$ erg s $^{-1}$, while type 2s have L_{Bol}^X in the range of $\sim 1.2 \times 10^{43}$ to $\sim 1.3 \times 10^{46}$ erg s $^{-1}$ with the median value $\sim 4.3 \times 10^{44}$ erg s $^{-1}$. The bolometric luminosities derived from the [OIII] luminosities ($L_{\text{Bol}}^{[\text{OIII}]}$) also span over similar range. The $L_{\text{Bol}}^{[\text{OIII}]}$ for type 1s spans over $\sim 1.0 \times 10^{43}$ to $\sim 6.2 \times 10^{46}$ erg s $^{-1}$ with the median value $\sim 4.4 \times 10^{44}$ erg s $^{-1}$, while for type 2s, it ranges from $\sim 4.4 \times 10^{44}$ to $\sim 1.3 \times 10^{46}$ erg s $^{-1}$ with the median value $\sim 1.0 \times 10^{45}$ erg s $^{-1}$. The two sample KS test shows that the two Seyfert subtypes of our sample have similar distributions of bolometric luminosities (L_{Bol}^X and $L_{\text{Bol}}^{[\text{OIII}]}$). There is $\sim 79\%$ and $\sim 99\%$ probability, respectively that the L_{Bol}^X and $L_{\text{Bol}}^{[\text{OIII}]}$ distributions of Seyfert type 1s and type 2s are drawn from the same parent population (Table 2). The similar distributions of the bolometric luminosities for the Seyfert type 1s and type 2s of our sample are in the lines as expected from the unification

scheme. The bolometric luminosities (derived from the X-ray as well as the [OIII] luminosities) for the Seyferts of our sample are in agreement with the ones reported in the previous studies (Ho 2009).

5.3. Comparison of black hole masses

Black hole mass is one of the fundamental parameters of AGN and if Seyfert type 1s and type 2s differ only due to the orientation of obscuring torus and host similar AGN, then, they are expected to have similar distributions of the supermassive black hole masses. We note that in our sample, black hole masses (M_{BH}) for Seyfert type 1s span over $\sim 3.2 \times 10^6$ to $\sim 1.2 \times 10^8 M_{\odot}$ with the median value $\sim 1.5 \times 10^7 M_{\odot}$, while for type 2s, it ranges from $\sim 1.4 \times 10^7$ to $\sim 7.4 \times 10^7 M_{\odot}$ with the median value $\sim 1.9 \times 10^7 M_{\odot}$. The comparison shows that the distributions of the black hole masses for the type 1s and type 2s of our sample are not significantly different (Figure 1), which is consistent with the unification scheme. The low p-value ~ 0.16 (Table 2) in the two sample KS test could be attributed to the small sample size. Our results are broadly in agreement with the previous studies (Panessa et al. 2006; Bian & Gu 2007; Middleton et al. 2008) which report that the black hole mass (M_{BH}) distributions are similar for Seyfert type 1s and type 2s.

5.4. Comparison of Eddington ratios

Eddington ratio ($\lambda = L_{\text{Bol}}/L_{\text{Edd}}$) *i.e.*, AGN bolometric luminosity normalized with Eddington luminosity can be used to characterize the level of nuclear activity (Ho 2008, 2009). For our sample sources we have two estimates of Eddington ratios *i.e.*, λ_X , where absorption-corrected 2.0 - 10 keV X-ray luminosity is used to estimate the AGN bolometric luminosity (L_{Bol}) and $\lambda_{[\text{OIII}]}$, where [OIII] luminosity is used to estimate L_{Bol} . Figure 4 shows the distributions of λ_X and $\lambda_{[\text{OIII}]}$ for the two Seyfert subtypes. We note that for the Seyfert type 1s, λ_X ranges from $\sim 6.3 \times 10^{-5}$ to $\sim 3.5 \times 10^{-1}$ with the median value $\sim 8.7 \times 10^{-3}$, while for type 2s, it ranges from $\sim 5.1 \times 10^{-4}$ to $\sim 6.2 \times 10^{-1}$ with the median value $\sim 2.0 \times 10^{-2}$. The two sample KS test shows that there is $\sim 98\%$ probability that the λ_X distributions of Seyfert type 1s and type 2s are drawn from the same parent population (Table 2). The distributions of $\lambda_{[\text{OIII}]}$ are also similar (p-value ~ 0.75) for the two Seyfert subtypes. For Seyfert type 1s, $\lambda_{[\text{OIII}]}$ spans over $\sim 7.6 \times 10^{-5}$ to $\sim 4.6 \times 10^{-1}$ with the median value $\sim 1.7 \times 10^{-3}$, while for type 2s, it spans over $\sim 1.9 \times 10^{-3}$ to $\sim 6.2 \times 10^{-1}$ with the median value $\sim 4.2 \times 10^{-2}$. The similar distributions of Eddington ratios for the two Seyfert subtypes implies that type 1s and type 2s have similar level of accretion and therefore, both the subtypes are intrinsically similar. Some of the literature studies have reported that the Seyfert type 2 galaxies accrete at lower Eddington ratios than type 1 Seyfert galaxies although black hole mass distributions for the two subtypes are similar (Panessa et al. 2006; Middleton et al. 2008). Our results are in contrary to these studies which report that the Seyfert type 2s are accreting at lower Eddington ratios in compared to type 1s. We note that while discussing the difference in the Eddington ratio distributions of the two Seyfert subtypes, Panessa et al. (2006) mention the points of caveats, *e.g.*, they used a constant correction factor to estimate the bolometric luminosity which may not be appropriate with the fact that the bolometric luminosity depends on the shape of the spectral energy distribution which could differ from high to low luminosity AGN

(Ho 1999; Marconi et al. 2004). Also, the absorption-corrected X-ray luminosity distributions for type 1s and 2s of their sample are substantially different which may consequently affect the distributions of Eddington ratios. Middleton et al. (2008) sample is based on hard X-ray observations *i.e.*, *INTEGRAL*-IBIS, *BeppoSAX*-PDS, *CGRO*-OSSE, and therefore it may be biased to towards relatively bright sources. Middleton et al. (2008) emphasized that Seyfert type 1s and type 2s need to be matched in intrinsic properties such as Eddington ratio in order to explore the orientation based differences. In fact, we follow the similar approach by using a sample in which two Seyfert subtypes are matched in orientation-independent properties (Lal et al. 2011).

Seyfert galaxies of our sample have Eddington ratios much lower compared to luminous AGNs (*i.e.*, quasars showing Eddington ratios $> 10^{-1}$ (Shemmer et al. 2006)) suggesting that the low luminosity of Seyfert AGN is likely due to low accretion rate. The AGN bolometric luminosities of the Seyfert galaxies (considering both the subtypes together) of our sample range from $\sim 8.7 \times 10^{42} \text{ erg s}^{-1}$ to $\sim 6.2 \times 10^{46} \text{ erg s}^{-1}$ with the median value of $\sim 3.6 \times 10^{44} \text{ erg s}^{-1}$. If this AGN emission is produced by a canonical optically thick, geometrically thin accretion disk (Shakura & Sunyaev 1973) that radiates at $L_{\text{acc}} = \eta \dot{M} c^2 = 5.7 \times 10^{45} (\eta/0.1) (\dot{M}/M_{\odot} \text{ year}^{-1}) \text{ erg s}^{-1}$ (see, Ho (2009)), then we expect a typical mass accretion rate in the range of $\dot{M} \sim 1.5 \times 10^{-3} - 11 M_{\odot} \text{ year}^{-1}$ with the median value of $6.3 \times 10^{-2} M_{\odot} \text{ year}^{-1}$, assuming radiative efficiency $\eta = 0.1$. Ho (2009) argued that the fuel required for the accretion rate $\dot{M} \sim 10^{-3} M_{\odot} \text{ yr}^{-1}$ can readily be supplied by the mass loss from evolved stars present in the bulge and the diffuse hot gas present in the circumnuclear region. The additional supply of fuel such as higher mass loss rates from the circumnuclear starburst, dissipation from larger scales nuclear bar or spirals and stellar tidal disruption is likely to present and therefore higher accretion rates are expected than that shown by low luminosity Seyferts. Radiatively inefficient accretion flows (RIAFs; (Narayan et al. 1998; Quataert 2001)) are generally invoked to explain the observed low Eddington ratios in low luminosity AGN. The relation between accretion rate and luminosity in RIAFs can be expressed as $\dot{m} \approx 0.7 (\alpha/0.3) (L_{\text{bol}}/L_{\text{Edd}})^{1/2}$, where $\dot{m} = \dot{M}/\dot{M}_{\text{Edd}}$ and α is viscosity parameter assumed to be $\approx 0.1 - 0.3$ (see, Ho (2009)). The Seyfert galaxies of our sample have $L_{\text{bol}}/L_{\text{Edd}} \sim 6.3 \times 10^{-5} - 6.2 \times 10^{-1}$ and this implies $\dot{m} \approx 1.9 \times 10^{-3} - 1.8 \times 10^{-2}$. These values of accretion rates lie well within the regime of optically thin RIAFs ($\dot{m} \leq \dot{m}_{\text{crit}} \approx \alpha^2 \approx 0.1$ (Narayan et al. 1998)).

6. Conclusions

- We have argued for the importance of sample selection in testing the predictions of the Seyfert unification scheme and showed that the distributions of the nuclear properties *i.e.*, the absorption-corrected 2.0 - 10 keV X-ray luminosities, the bolometric luminosities, the black hole masses and the Eddington ratios are similar for the two Seyfert subtypes of a sample based on orientation-independent properties. Our results on the statistical comparison of the nuclear properties of the Seyfert type 1s and type 2s are consistent with the orientation and obscuration based Seyfert unification scheme.
- The absorption-corrected 2.0 - 10 keV X-ray luminosities are in the range of $\sim 10^{42} - 10^{44} \text{ erg s}^{-1}$ for both the Seyfert subtypes, with similar median values. The estimated bolometric luminosities derived from the X-ray as well as the [OIII] luminosities are in range of $\sim 10^{43} - 10^{46} \text{ erg s}^{-1}$ for both the Seyfert subtypes, with similar median values.

- Both the Seyfert subtypes accrete with sub-Eddington rates *i.e.*, Eddington ratios range $\sim 10^{-4} - 10^{-1}$ in compared to luminous AGNs (*e.g.*, quasars with Eddington ratio ~ 1). The plausible explanation for the substantially low Eddington ratios may be the radiatively inefficient accretion such as advection dominated accretion flow and their variants (Narayan & Yi 1994).

References

- Antonucci, R. 1993, ARA&A, 31, 473
 Antonucci, R. 2002, in ASPC, Vol. 284, IAU Colloq. 184: AGN Surveys, ed. R. F. Green, E. Y. Khachikian, & D. B. Sanders, 147
 Antonucci, R. R. J. & Miller, J. S. 1985, ApJ, 297, 621
 Awaki, H., Koyama, K., Inoue, H., & Halpern, J. P. 1991, PASJ, 43, 195
 Bassani, L., Dadina, M., Maiolino, R., et al. 1999, ApJS, 121, 473
 Beckmann, V., Soldi, S., Ricci, C., et al. 2009, A&A, 505, 417
 Bian, W. & Gu, Q. 2007, ApJ, 657, 159
 Brightman, M. & Nandra, K. 2011, MNRAS, 413, 1206
 Buchanan, C. L., Gallimore, J. F., O’Dea, C. P., et al. 2006, AJ, 132, 401
 Capri, M., Panessa, F., Bassani, L., et al. 2006, A&A, 446, 459
 Dadina, M. 2008, A&A, 485, 417
 Dasyra, K. M., Tacconi, L. J., Davies, R. I., et al. 2006, ApJ, 651, 835
 Elvis, M., Wilkes, B. J., McDowell, J. C., et al. 1994, ApJS, 95, 1
 Ferrarese, L. & Merritt, D. 2000, ApJ, 539, L9
 Gebhardt, K., Bender, R., Bower, G., et al. 2000, ApJ, 539, L13
 González Delgado, R. M., Heckman, T., Leitherer, C., et al. 1998, ApJ, 505, 174
 González-Martín, O., Masegosa, J., Márquez, I., & Guainazzi, M. 2009, ApJ, 704, 1570
 Hasinger, G. 2008, A&A, 490, 905
 Heckman, T. M., Gonzalez-Delgado, R., Leitherer, C., et al. 1997, ApJ, 482, 114
 Heckman, T. M., Kauffmann, G., Brinchmann, J., et al. 2004, ApJ, 613, 109
 Heckman, T. M., Ptak, A., Hornschemeier, A., & Kauffmann, G. 2005, ApJ, 634, 161
 Ho, L. C. 1999, ApJ, 516, 672
 Ho, L. C. 2008, ARA&A, 46, 475
 Ho, L. C. 2009, ApJ, 699, 626
 Ho, L. C. & Ulvestad, J. S. 2001, ApJS, 133, 77
 Horst, H., Gandhi, P., Smette, A., & Duschl, W. J. 2008, A&A, 479, 389
 Kaspi, S., Smith, P. S., Netzer, H., et al. 2000, ApJ, 533, 631
 Kauffmann, G. & Heckman, T. M. 2009, MNRAS, 397, 135
 Kellermann, K. I., Sramek, R., Schmidt, M., Shaffer, D. B., & Green, R. 1989, AJ, 98, 1195
 Lal, D. V., Shastri, P., & Gabuzda, D. C. 2011, ApJ, 731, 68
 Lamastra, A., Bianchi, S., Matt, G., et al. 2009, A&A, 504, 73
 Laor, A. 2003, ApJ, 590, 86
 Levenson, N. A., Heckman, T. M., Krolik, J. H., Weaver, K. A., & Życki, P. T. 2006, ApJ, 648, 111
 Levenson, N. A., Weaver, K. A., Heckman, T. M., Awaki, H., & Terashima, Y. 2004, ApJ, 602, 135
 Malkan, M. A., Gorjian, V., & Tam, R. 1998, ApJS, 117, 25
 Marconi, A., Risaliti, G., Gilli, R., et al. 2004, MNRAS, 351, 169
 Merloni, A., Heinz, S., & di Matteo, T. 2003, MNRAS, 345, 1057
 Middleton, M., Done, C., & Schurch, N. 2008, MNRAS, 383, 1501
 Moran, E. C., Barth, A. J., Kay, L. E., & Filippenko, A. V. 2000, ApJ, 540, L73
 Mulchaey, J. S., Koratkar, A., Ward, M. J., et al. 1994, ApJ, 436, 586
 Narayan, R., Mahadevan, R., & Quataert, E. 1998, in Theory of Black Hole Accretion Disks, ed. M. A. Abramowicz, G. Björnsson, & J. E. Pringle, 148
 Narayan, R. & Yi, I. 1994, ApJ, 428, L13
 Nicastro, F. 2000, ApJ, 530, L65
 Panessa, F. & Bassani, L. 2002, A&A, 394, 435
 Panessa, F., Bassani, L., Capri, M., et al. 2006, A&A, 455, 173
 Quataert, E. 2001, in ASPC, Vol. 224, Probing the Physics of Active Galactic Nuclei, ed. B. M. Peterson, R. W. Pogge, & R. S. Polidan, 71
 Ricci, C., Walter, R., Courvoisier, T., & Paltani, S. 2011, ArXiv e-prints
 Risaliti, G., Maiolino, R., & Salvati, M. 1999, ApJ, 522, 157
 Schmidt, M. & Green, R. F. 1983, ApJ, 269, 352
 Schmitt, H. R., Donley, J. L., Antonucci, R. R. J., et al. 2003, ApJ, 597, 768
 Shakura, N. I. & Sunyaev, R. A. 1973, A&A, 24, 337
 Shemmer, O., Brandt, W. N., Netzer, H., Maiolino, R., & Kaspi, S. 2006, ApJ, 646, L29
 Singh, V., Shastri, P., & Risaliti, G. 2011, A&A, 532, A84+
 Smith, D. A. & Done, C. 1996, MNRAS, 280, 355
 Spinoglio, L. & Malkan, M. A. 1989, ApJ, 342, 83
 Taylor, G. B., Silver, C. S., Ulvestad, J. S., & Carilli, C. L. 1999, ApJ, 519, 185
 Tran, H. D. 2001, ApJ, 554, L19

- Tran, H. D. 2003, *ApJ*, 583, 632
- Treister, E., Urry, C. M., & Virani, S. 2009, *ApJ*, 696, 110
- Tueller, J., Mushotzky, R. F., Barthelmy, S., et al. 2008, *ApJ*, 681, 113
- Turner, T. J., George, I. M., Nandra, K., & Mushotzky, R. F. 1997, *ApJS*, 113, 23
- Ueda, Y., Akiyama, M., Ohta, K., & Miyaji, T. 2003, *ApJ*, 598, 886
- Urry, K., Padovanni, G., Wilson, A. S., & Yoshida, M. 1995, *ApJ*, 521, 565
- Wang, J., Mao, Y. F., & Wei, J. Y. 2009, *AJ*, 137, 3388
- Wang, J. & Zhang, E. 2007, *ApJ*, 660, 1072
- Weedman, D. W. 1977, *ARA&A*, 15, 69
- Wilson, A. S. 1996, *Vistas in Astronomy*, 40, 63
- Woo, J. & Urry, C. M. 2002, *ApJ*, 579, 530